Maritime Technology and Engineering 3 – Guedes Soares & Santos (Eds)
© 2016 Taylor & Francis Group, London, ISBN 978-1-138-03000-8

Ship resistance and flow field around the KVLCC2 hull

S. Tarbiat & C. Guedes Soares
Centre for Marine Technology and Ocean Engineering (CENTEC), Instituto Superior Técnico, Universidade de Lisboa, Lisbon, Portugal

ABSTRACT: An open source CFD solver has been adopted to calculate ship resistance and flow field at the propeller position of the KVLCC2 hull. The SST k–ω viscosity model used to predict the forces around hull. Free surface is captured using the VOF (volume of fluid) method. The ship hull is free to perform heave and pitch motions, so the trim effect on the hull resistance is also considered. The output results include resistance and flow field at the propeller position, which are compared against experimental data and also other numeric results. Iterative and parameter convergence studies are conducted using systematic parameter refinement to estimate numerical errors and uncertainties on resistance results. It is found that the ship resistances, velocity at the stern and wave profile around the hull are in a very good agreement against experimental data.

1 INTRODUCTION

Computational fluid dynamic approaches are based on the solution of Reynolds Averaged Navier-Stokes equation (RANS) overcoming the potential flow limitations. RANS predictions in addition to providing the ship motion and resistance information, can also predict flow field information, which is useful for ship design optimization. Flow field prediction around the ship hulls using RANS started in the 1980s, and most studies focused on the flow field in steady state.

This paper focus on CFD calculations of the resistance of the KVLCC2 hull in 1/58th model scale. This hull has been used as benchmark by various authors and there are several investigations performed both experimentally and numerically on this ship model. Experiments on this model in towing tank were done by Van et al. (1998). Resistance calculation in calm water and also wave pattern in towing tank was measured by Kim et al. (2001) which is one of the best validation cases for CFD simulations for this hull. Guo et al. (2010, 2013) worked on both experimental measurement and CFD calculations of resistance in calm water and also in waves. Malin (2013) also studied calm water simulations in both FINE/Marine and Star-CCM+, and these results were then compared to results achieved in simulations that included different kinds of waves. To obtain the distribution of turbulence statistics, Lee et al. (2003) focused on flow information in the stern and wake regions of ship model in a wind tunnel.

One of the challenging subjects in CFD simulations is the selection of the turbulence model. Three types of turbulence models namely RSM, k–ε models and k–ω models were tested by Svennberg (2000) to identify the flow behavior around the KVLCC2 hull. The RSM and SST models gave the best results in comparison with experiments.

One of the main sources of benchmarks for CFD computations is the Gothenburg 2000 workshop, which was an international benchmark workshop for computational fluid dynamics applied to ship flows. For resistance coefficient prediction the k–ε models, k–ω models, RSM and algebraic stress models were used, which shows that based on various viscous models ship resistance is different. (Larsson et al., 2003).

In the past, most researches were performed in steady state conditions, while in recent years there are more efforts on simulations with waves. For instance, Deng et al. (2009) investigated short waves cases for a container ship and Deng, et al. (2010) studied the resistance in waves for a KVLCC2 hull using the ISIS-CFD flow solver.

Most of the studies did not consider the effect of free surface flow, while in this study the free surface effect is considered to predict the flow field around the ship hull. Here an open-source solver is used to predict forces and moments for the ship hull for the straight course while the flow passes along the hull. Also the flow fields for the KVLCC2 at different positions are studied and compared against experiments data, and finally trim and heave effects on results investigated. The outputs include hull resistance, wave profiles around the ship hull and among computational domain as well as numerical convergence study on resistance results.

2 NUMERICAL METHODS

OpenFOAM contains a suite of numerical tools to solve the fluid behavior around a ship hull. The present

study used RANS based LTSInterFoam and interDyM-Foam solvers which are widely used for evaluation of hull form resistance and ship motions. The VOF (Volume of Fluid) method is used as a scalar indicator function to represent the phase of the fluid in each cell. The governing equations are shown as follows:

$$\frac{\partial u_i}{\partial x_i} = 0 \tag{1}$$

$$\frac{\partial u_i}{\partial x_i} + \frac{\partial (u_i u_j)}{\partial x_j} = -\frac{1}{\rho}\frac{\partial P}{\partial x_i} + \frac{\partial}{\partial x_j}\left(\gamma \frac{\partial u_i}{\partial x_j}\right) - \frac{\partial}{\partial x_j}\overline{\acute{u}_i \acute{u}_j} + g_i \tag{2}$$

where u_i, u_j are average speed components, ρ is the density of fluid, P is the average pressure, γ is the coefficient of kinematic viscosity, g_i is the gravity acceleration, and $\frac{\partial}{\partial x_j}\rho\overline{\acute{u}_i \acute{u}_j}$ is the Reynolds stress. The unknown term of Reynolds stress can be solved by using additional equations. The SST k—ω model is applied with free water surface model by the VOF method. The LTSInterFoam solver (local-time stepping interFoam) in OpenFOAM, first maximizes the time-step according to the local Courant number and then processes the time-step field by smoothing the variation in time step across the domain to prevent instability due to large conservation errors caused by sudden changes in time step. The InterDyMFoam solver, which uses a VOF (volume of fluid) phase-fraction based interface capturing approach, with mesh motion is also used, to consider the effect of trim and heave motions in the present simulations.

3 GRID GENERATION

Four different mesh sizes are used to investigate grid convergence, using 0.4M, 0.7M, 1.1M and 2.1M cells. As the ship hull model is a complicated one, it is difficult to refine the mesh systematically for each direction. Here the mesh is refined for four cases as systematically as it can be.

It should be also noted that the main region that is refined is the free surface, or the interface between the air and water. This is possibly the most important one, because of how these two fluids interact due to the difference in their properties. Figure 1 and 2 present the grids generated by snappyHexMesh tool in OpenFOAM for the case with 1.1M number of cells which is selected for this study. The distance y+ at the wall-adjacent cell is kept in the range of 20–40 and the mesh is produced with snappyHexMesh tool in OpenFOAM.

The computational domain is shown in Fig. 2. Only half of the ship is modeled, in order to exploit the symmetry of the flow. The domain extent as follow:

$$-3.0Lpp < x < 2.5Lpp\,, 0.0L\,pp < y < 2.5L\,pp \;and\; -1.6Lpp < z < 0.5Lpp \tag{3}$$

where Lpp is the length between perpendiculars. The water level fixed at $z = 0.3586$ which is equal to the scaled model draft.

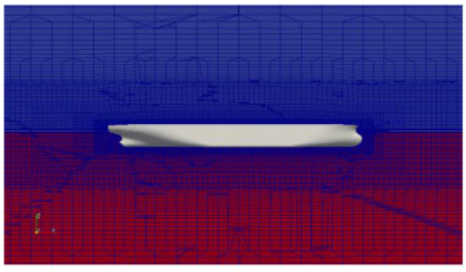

Figure 1. Grid around KVLCC2 hull.

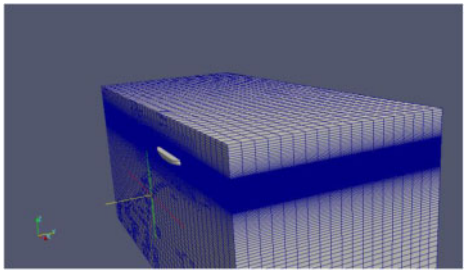

Figure 2. Grid on computational domain.

'Velocity inlet' is provided at the inlet boundary condition, 'Pressure outlet' is provided at the outlet boundary. For the other boundaries include bottom, sides and atmosphere 'Symmetry' boundary is used. To see if the simulation have converged the residuals of the total resistance coefficient are examined and plotted in figure 3 and it shows that resistance calculations converged after 3000 seconds.

4 CONVERGENCE STUDY

The convergence study of the RANS simulations is very important for the application of CFD methods due to the diverse methods for numerical simulations, complex geometries and also free-surface effect. Verification and validation methods are used in this study to estimate errors due to the iteration, mesh and other parameters changing. Verification methods are proposed based on Richardson extrapolation.

As the grid size and time step decrease to zero, the discretization error should tend to zero. A procedure where the grids are refined systematically is often referred as a grid convergence study, which can decrease the level of discretization error of the numerical result. The application of grid convergence and iterative convergence analysis on KVLCC2 calm water results will be discussed here.

The total resistance of a ship hull is decomposed into frictional resistance and viscous pressure resistance. In this study, the free surface effect is taken into account and the total resistance on ship hull is calculated using different grids. Table 1 shows the total resistance around hull using different grids.

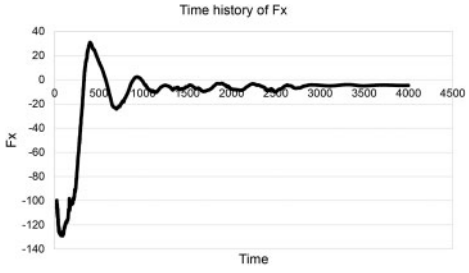

Figure 3. Total resistance convergence study.

Table 1. Hull resistance at Fn = 0.142 using different grids.

	Case 4	Case 3	Case 2	Case 1
	Coarse	Medium	Fine	Finest
$C_T \times 10^3$	4.616	4.291	4.199	4.160

Table 2. Convergence ratios for each three cases among four cases.

	Case 1,2,4	Case 1,3,4	Case 2,3,4	Case 1,2,3
R_G	0.09352	0.40307	0.28307	0.42391

It is obvious from the table 1 that the ship resistance decreases with increasing mesh. From case 3 to $2,5 \times 10^5$ number of cells are increased while the estimated error decreases 2.23%. From case 2 to 1, with the two times more increase in the number of cells, the estimated error decreased to 1%, which shows a good accuracy.

It should be noted that the mesh refinement is not uniform as the ship hull is very complicated and the mesh refined around the hull and free surface locally.

4.1 *Grid convergence study*

In this part, the grid convergence study is performed for the ship resistance coefficient at the design speed. Here, verification methods by Stern et al. (1998) are used. As there are four grid cases given here, any three of them can be chosen for the convergence study. For each three cases the relevant convergence ratios are shown in Table 2.

The results for convergence ratios show that for any combination of the grids there are monotonic convergence as R_G (convergence ratio) is between 0 and 1, so the generalized Richardson extrapolation can be used to calculate numerical uncertainty U_G.

In this study the methodology by Stern et al. (2004) is applied on two groups of results which give the results in Table 3.

The first combination group gives an order of accuracy equal to $P_G = 7.626$, while the second grid group gives $P_G = 8.371$.

Table 3. Verification study of resistance coefficient.

Grid	R_G	r_{G21}	r_{G32}	P_G	$\delta_{RE,G1}$	F_S	U_G
Case 1,3,4	0.40307	1.4683	1.1717	7.626	0.00739	1.25	0.00924
Case 2,3,4	0.28307	1.2006	1.1717	8.371	0.02541	1.25	0.03176

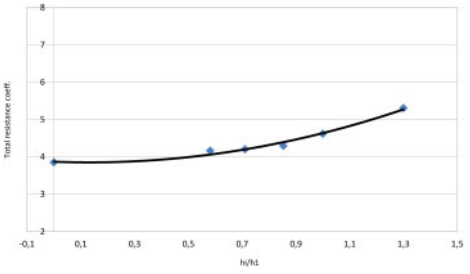

Figure 4. Grid convergence of the total resistance.

Table 4. Verification study of resistance coefficient.

	P_G	$\emptyset_0$	U_S	U_G
C_t	6.590	3.9	0.20%	2.33%

Uncertainty is estimated using the generalized Richardson extrapolation with safety factor. The exact value for the safety factor should be decided by experience; in this study Roache (1994) recommendation for safety factor has been used (1.25).

As the experimental uncertainty data is not available, in this study the convergence study of numerical results is used to verify the numerical model.

As the ship hull model is a complicated one, it is difficult to refine the mesh systematically for each direction. Here the mesh refined for four cases as systematically as it can be.

Numerical results of total resistance coefficient versus the refinement ratio h_i/h_1 are shown in Figure 4. Curves fitted to results on total resistance to obtain extrapolated solution $\emptyset_0$.

The observed order of accuracy for the finest combination groups, the extrapolated solution, standard deviation, and uncertainty are all listed in Table 4.

4.2 *Iterative convergence study*

KVLCC2 hull is a complex geometry, so the solution residual drop to 10^{-4} range for the finest grid. For iterative error and uncertainty estimation the ship resistance plotted against history time of simulation. The iterative history of total resistance coefficient for finest mesh is shown in Figure 5.

From time history it can be seen that the amplitude results decreased with the iteration increase.

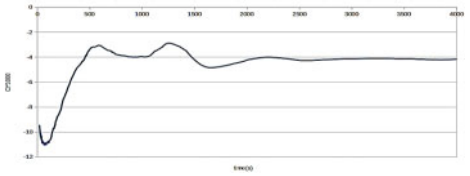

Figure 5. Ship resistance coefficient time history for case 1.

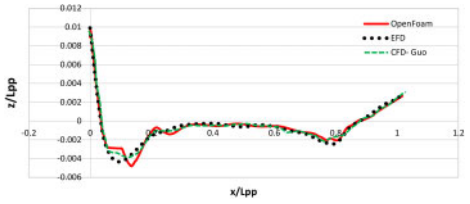

Figure 6. Free surface wave elevation along the hull.

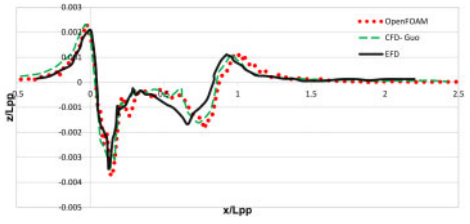

Figure 7. Wave profile at y/Lpp = 0.0964.

The solution is mixed convergence/oscillatory iterative convergent. The iterative error can be defined by

$$U_I = {}^1/_2\,(S_U - S_L) \tag{4}$$

As is shown in figure 1, the maximum solution envelope is $S_U = -4.1458$ and the minimum is $S_L = -4.1632$, so the iterative error can be calculated as

$$U_I = {}^1/_2\,(S_U - S_L) = 0.0087 \tag{5}$$

5 RESULTS AND DISCUSSION

In this study to model the free surface in viscous flow, the surface capturing method (VOF) is used. The wave elevation around the ship is given in figure 6. Experimental data by Kim, et al. (2001) has been used for validation of numerical results here.

From figure 6, it is obvious that the differences between EFD and CFD results are very small and it can be concluded that LTSInterFoam is suitable to model free surface. Also the wave cuts in two more places are shown in figures 7 and 8. It is clear that the wave profile is predicted well near the ship, while it is not good for far regions and it is reasonable as the mesh is coarse in these regions.

Moreover, the flow field at the propeller position is studied in this paper. As the flow field is important

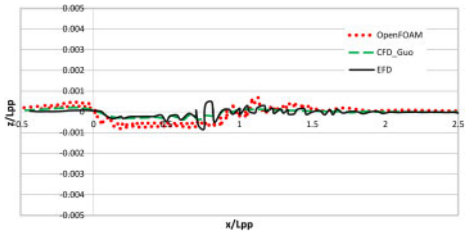

Figure 8. Wave profile at y/Lpp = 0.2993.

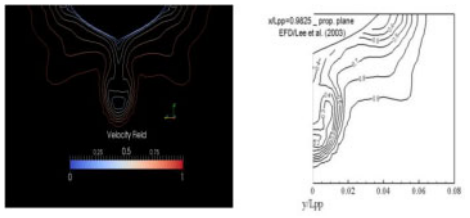

Figure 9. Velocity field at x/Lpp = 0.9825 (Left-OpenFOAM, Right-Experimental).

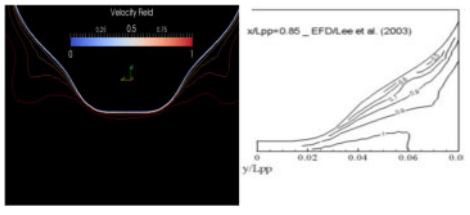

Figure 10. Velocity field at x/Lpp = 0.85 (Left-OpenFOAM, Right-Experimental).

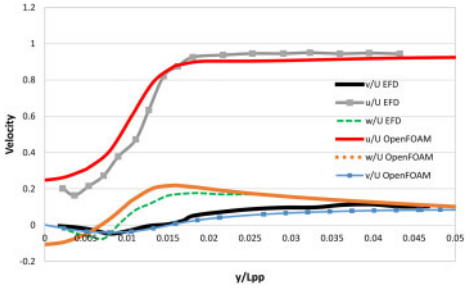

Figure 11. Velocity profile at propeller position along z/Lpp = −0.05075.

while the propeller is working it has an important role in prediction of turbulent flow around the ship. The velocity contour in the propeller position compared against experimental data shows a good agreement. Figure 9 shows the axial velocity contours at the propeller position.

For further investigation the flow near the propeller plane at x/L pp = 0.85 is given in figure 10 which shows numerical results compared to EFD.

Figure 11 indicates the mean velocity profile components at the propeller position. The velocity profiles

Table 5. KVLCC2 hull resistance at Fn = 0.142 using different grids.

	Case 4 Coarse	Case 3 Medium	Case 2 Fine	Case 1 Finest
Mesh sizes	420220	676110	1170128	2140260
$C_T \times 10^3$	4.616	4.291	4.199	4.160
Error%	12.311	4.403	2.165	1.201

Table 6. KVLCC2 resistance, sinkage and trim comparison against model test.

	OpenFOAM LTSInterFoam	OpenFOAM interDyMFoam	Model tests (Guo)
Speed [m/s]	1.047	1.047	1.047
Froud Number	0.142	0.142	0.142
Sinkage [mm]	–	−5.210	−6.419
Pitch [degrees]	–	−0.112	−0.126
Resistance [N]	18.23	18.22	18.20

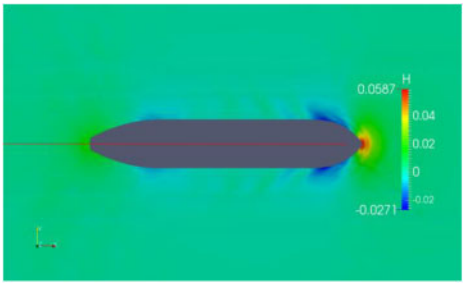

Figure 12. Wave pattern in calm water, Fn = 0.142.

from numerical results are close to the experiment results.

The total resistance around the ship hull for three types of meshes is now presented. Most of the previous calculations for KVLCC2 neglected the effects of free surface, while here the free surface is taken into account and the total drag forces is calculated for different grids. Table 5 shows the results for total resistance coefficient calculated with SST k–ω. The ship resistance decreases with the increase of the mesh.

Total resistance forces, sinkage and pitch changes for the 1.1M cells are presented in table 6, together with the comparison by model tests values by Guo (2010). As it is clear from the table, the results are alike and the differences are very small for calm water simulations.

Finally Figure 12 shows the wave pattern along the computational domain. It can be seen that how the wave patterns differs near the ship hull.

Also from table 6 it is obvious that the results for resistance using two types of solvers (LTSInterFoam and interDyMFoam) are very close to each other, so considering the effect of trim and heave can only have a small effect on KVLCC2 resistance. It can be concluded from these results for current case, dynamic trim and sinkage are not important for the results.

6 CONCLUSIONS

Numerical simulations of KVLCC2 hull in calm water have been performed. Results include ship total resistance, flow field at the propeller position and two more positions in the stern and wave patterns around the hull. The ship hull was free to heave and pitch and three types of grids are studied in this paper. The following conclusions are extracted:

The total resistance and flow field at the propeller field is predicted well and the wave profile around the hull is well captured in the simulation. The wave field around the hull is well captured, while it is not so good for far regions but the mesh is coarse in these regions.

By comparing results using two types of solvers, LTSInterFoam and interDyMFoam it can be concluded that the trim and sinkage have small effect on the resistance and can be neglected. As the LTSInterFoam is faster, they are preferable for this specific case (KVLCC2) hull in forward speed.

A systematic analysis of numerical convergence of the resistance of the KVLCC2 hull is performed as well as an iterative convergence study.

The three finest groups of grids provide smaller accuracy in comparison with the other group. The order of convergence approaches the theoretical one, as the grids get fine enough, which shows that the OpenFOAM results are convergent. Also from the time history of the total ship resistance it is clear that the amplitude of the solution envelope decreases as the iteration number increases.

ACKNOWLEDGEMENTS

The work is a part of the SHOPERA (Energy Efficient Safe SHip OPERAtion) collaborative project which is co-funded by the Research DG of the European Commission within the RTD activities of the FP7 Thematic Priority Transport/ FP7-SST-2013-RTD-1.

REFERENCES

Deng, G.B. Queutey, P. & Visonneau, M. 2010. RANS prediction of the KVLCC2 tanker in head waves. Journal of Hydrodynamics, Ser. B. 476–481.

Deng, G.B. Queutey, P. Visonneau, M. 2009. Seakeeping Prediction for a Container Ship With RANS Computation. 22nd Chinese conference on hydrodynamic. Chengdu. China.

Fureby, C. Toxopeus, S.L. Johansson, M. Tormalm, M. Petterson, K. 2016. A computational study of the flow around the KVLCC2 model hull at straight ahead conditions and at drift. Ocean Engineering. 118:1–16.

Guo, B. & Steen, S. 2010. Added Resistance of A VLCC in short waves. Proceedings of OMAE 2010. Shanghai. China. pp. 609–617.

Guo, B. & Steen, S. 2010. Computational study on ship resistance and flow field of kVLCC2. Gothenburg 2010 A workshop on Numerical Ship Hydrodynamics. Department of Marine Technology. NTNU. Norway.

Guo, B.J. Deng, G. B. & Steen, S. 2013. Verification and validation of numerical calculation of ship resistance and flow field of a large tanker. Ships and Offshore Structures. 8:1. 3–14.

Kim, W.J. Van, S.H. & Kim, D.H. 2001. Measurement of flows around modern commercial ship models. Experiments in Fluids. Vol. 31. pp. 567–578.

Larsson, L. Stern, F. & Bertram, V. 2003, Benchmarking of Computational Fluid Dynamics for Ship Flows. Gothenburg 2000 Workshop. Journal of Ship Research. Volume 47. No. 1, pp. 63–81.

Lee, S.J. Kim, H.R. Kim, W.J. & Van, S.H. 2003. Wind Tunnel Tests on Flow Characteristics of the KRISO 3600 TEU Containership and 300K VLCC Double-Deck Ship Models. Journal of Ship Research. Vol.47. No.1. pp. 24–38.

Malin, S. 2013. Application of CFD to seakeeping. Master thesis. Department of Marine Technology. NTNU. Norway.

Roache, P. 1994. Verification and Validation in Computational Science and Engineering. Hermosa Publishers. Albuquerque.

Stern, F. & Longe, J. 1998. Evaluation of Surface-Ship Resistance and Propulsion Model-Scale Database for CFD validation. Proceeding of the 1st Symposium on Marine Application of CFD. McLean. VA.

Stern, F. Wilson, R. & Shao, J. 2004. Quantitative V&V of CFD Simulations and Certification of CFD Codes with Examples. Proceeding of CHT-04 ICHMT International Symposium on Advances in Computational Heat Transfer. Norway.

Svennberg, S.U. 2000. A test of turbulence models for steady flows around ships. Gothenburg 2000 a workshop on numerical ship hydrodynamics. Gothenberg. Sweden.

Toxopeus, S.L. Simonsen, C.D. Guilmineau, E. Visonneau, M. Xing, T. Stern, F. 2013. Viscous-flow calculations for KVLCC2 in manoeuvring motion in deep and shallow water. J. Mar. Sci. Technol. 18:471–497.

Van, S.H. Kim, W.J. Yim, G.T. Kim, D.H. & Lee, S.J. 1998. Experimental Investigation of the Flow Characteristics Around Practical Hull Forms. Proceedings 3rd Osaka Colloquium on Advanced CFD Applications to Ship Flow and Hull Form Design. Osaka. Japan.

Weymouth, G. Wilson, R. & Stern, F. 2005. Prediction of Pitch and Heave Ship Motions in Head Seas. Journal Ship Research. 49(2): 80–97.